Deliverable 7.6: Report on the performance of the 500W Demonstrator (3D & Si processing (2))

Dissemination Level: Public

Owner	
Name:	Gerhard Kunz
Lead Beneficiary:	BOSCH
Phone:	+49 711 811 24266
E-mail:	Gerhard.Kunz@de.bosch.com
Context	
Author(s):	Gerhard Kunz (BOSCH), Daniel Holder (USTUTT), David Bruneel (LASEA)
Work Package:	WP 7
Task:	T 7.4.1
Document Status	
Version:	1.00
Last modified:	30/08/2019
Status:	Final
Approved by:	Marwan Abdou Ahmed
Date Approved:	30/08/2019

Declaration: Any work or result described therein is genuinely a result of the Hiperdias project. Any other source will be properly referenced where and when relevant

Contents

1 Introduction

The requirements to reach have been defined in the D1.2. They have driven the development of the different components of the demonstrator, including the laser. The mechanics, electrics and the optics and the different components to be used have been defined and chosen with the requirements as a target pushing the technics beyond what already exists in the laser machine world. For example the use of a very high power laser made impossible to use a standard f-theta lens as this would damage the galvo mirrors. To overcome this the focusing has been decided to be done before the galvo mirrors with the varioscan, implying to use calibration files in a nonstandard way. The optics and the control of the galvo scanner combined with the varioscan had to be designed in order to reach the requested spot size. This new concept of demonstrator has been completed and delivered to USTUTT where the tests and the upscaling will take place. The demonstrator of 500W has been evaluated by the end-user (BOSCH) this evaluation is reported here.

1.1 KPI's used for evaluation

For the purpose of a quantitative evaluation of quality and productivity criteria, specific KPI's have been developed in the scope of D1.2. They are listed in Table 1 including a (maximum) target value that are necessary in order to realize the later product functionality and to meet the strict requirements for a mass manufacturing of high-precision products such as sensors and Microelectromechanical systems (MEMS). The KPI's were used to track progress and status of the development state during fundamental process development using up to 50 W of average laser power and the later upscaling using up to 500 W of average laser power. In this previous work, rectangular ablation geometries were used for evaluation. In contrast to this, within the context of this deliverable, the results were evaluated on the basis of the demonstrator geometry, which exhibits the relevant features of later products.

Table 1: Bosch KPI's: Definition and limit values

Key Performance Indicator	Symbol	Unit	Target Value
KPI1: average ablation rate	$\bar{V}$	mm³/s	≥1
KPI2: peak ablation rate	$\dot{V}_{max}$	mm³/s	≥3
KPI3: shape deviation	δ_S	µm	≤10 (waviness)
KPI4: average surface roughness	S_a	µm	≤1
KPI5: thickness of surface damage	$l_{d,sd}$	µm	≤1
KPI6: Surface defects > 1 µm	–	1/mm²	none
KPI7: min. achievable edge radius	r_e	µm	≤ 200
KPI8: max. edge-steepness	α_e	degree	≥ 70

1.2 Key aspects regarding laser system

Experiments were designed with the objective to identify process limits and parameters that allow achievement of the KPI's. The required set of parameters was established according to the findings from the fundamental process development (WP2), performed with several USP lasers with low/medium

average power of up to 50 W. Those parameters were translated into the system requirements listed in Table 2.

Table 2: Parameters and system requirements for the HIPERDIAS-Demonstrator defined in WP2, actual value of parameters of the 500 W demonstrator @ IFSW and evaluation of fulfilment regarding requirements

Parameter	Dim.	Min. Spec. (to achieve project goal)	Desirable Spec.	1st demonstrator @ IFSW	fulfilment
Focal spot diameter	µm	*50* … 200	*50* … 200	Approx. 96	fulfilled
Average power	W	> 1000	> 1000	430	sufficient for 1st demonstrator
Pulse repetition rate	kHz	< 2000	*< 1000*	1250	fulfilled
Scan velocity	m/s	> 4	> 8	Max.: > 30 m/s	fulfilled
Pulse duration	ps	0,4 … 10 (fix)	*0,4 … 10 (variable)*	< 300 (fix)	fulfilled
Pulse energy	µJ	> 500	> 500	351	sufficient for 1st demonstrator
Roundness beam profile (focal)	%	*80*	*90*	See Figure 1	sufficient for 1st demonstrator
Sattelite spots	-	*None*	*None*	None	fulfilled
M²	-	*< 10*	*< 5*	< 1.3	fulfilled
Wavelength		*IR*	*IR*	IR	fulfilled
Number of Pulses per Burst	-	> 2	***10***	8	fulfilled
Temporal intra-burst distance	ns	***20 … 80***	***10 … 150***	25 ns fix	fulfilled
Intensity level of burst pulses / burst	-	***equal***	***Individually adjustable***	Nominally equal; variations @ low number of pulses/burst (1…5) → Bosch: 20% variation w.r.t. nominal acceptable	fulfilled

Synchronization: Scan velocity & laser reprate (pulse on demand)	-	Yes	Yes	Not implemented	sufficient for 1st demonstrator
Synchronization: Scan position & pulse energy (amplitude o. d.)	-	No	***Yes***	Not implemented	Optional requirement
Admissible focus shift	-	***< 2 * r.l***	***< 1 * rayleigh l.***	< 1 * rayleigh length	Not measured
Polarization @ workpiece	-	***Circular***	***Adjustable circular / linear***	Adjustable circular / linear	Not measured
User Interface		***Graphical, established Scanning software***		KAYLA-Software by LASEA for Machine, seperate GUI for amplitude laser	fulfilled
Machine Vision (Camera)	-	***Overview***	***Overview + Detail***	Overview camera (not integrated in system software) + detail measurement e.g. OCT, integrated in system SW)	fulfilled

It was taken into account that the upscaling, meaning the increase of average power up to 1 kW and pulse energy in order to achieve higher productivity, most likely doesn't show linear behavior. It was expected that there are losses due to unknown effects that may occur as silicon is ablated with a femtosecond ultra short pulse laser in this power range.

Therefore, first trials were performed within the scope of WP2 to test the applicability of this parameters and requirements at the partner IFSW. As a result it was shown that good surface quality is achievable using high average power and pulse energy. Furthermore, it was concluded that thermal effects are very relevant, as they not only can lead to surface deterioration but also can cause wafer breakage. Due to this, the application of average power was identified as the main challenge in order to achieve the KPI's and the project goal. As can be obtained from Table 2, the 500 W- Demonstrator has an average power of 430 W. Although this is not as much as planned, it is possible to investigate the ablation process and relevant effects. Furthermore, the additionally defined burst functionality is implemented as it was identified to be decisive for quality and productivity of the ablation process.
Specifications such as polarization, focus shift or the synchronization of the scan velocity with the laser repetition rate play a rather less important role for the 500 W demonstrator and can be evaluated with the 1000 W demonstrator.

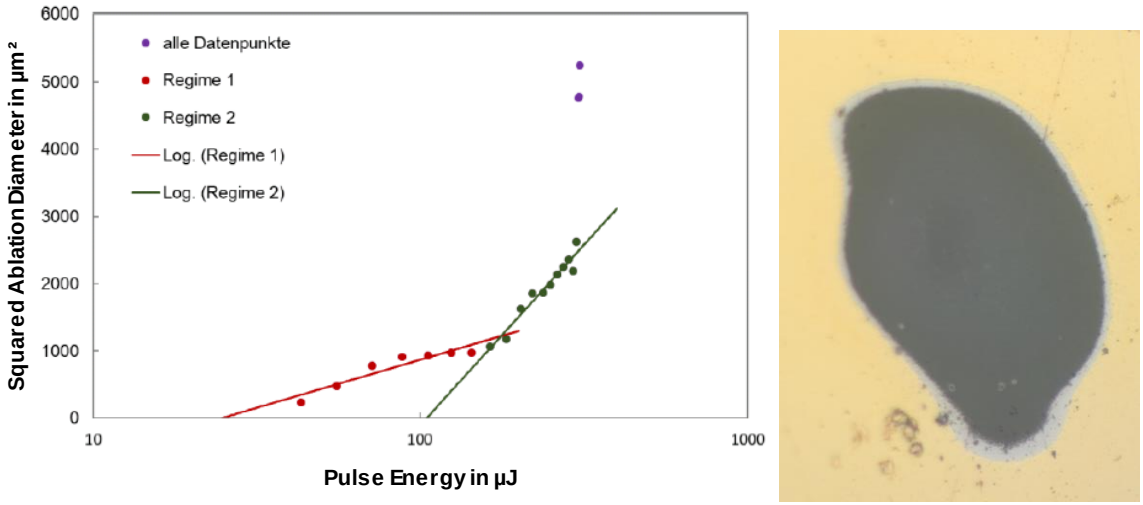

Figure 1: Experimental results of the determination of the spot diameter using the method by LIU[1] (left), ablation crater as result of single-pulse ablation on silicon (right).

Special attention is paid to the roundness and diameter of the focused laser beam in the focal plane. As depicted in Figure 1 (right), the crater that is ablated from silicon with a single laser pulse is shaped irregularly. From this it can be derived that the intensity distribution is also irregular which leads to the assumption that the M^2 is greater than at its initial measurement, performed directly after the implementation of the laser system. Due to this, it is difficult to precisely identify the value of the focal diameter: Using the method by LIU[1] presuming a regular shape and a gaussian intensity distribution, a spot diameter of d_f = 35,8 µm can be determined. This is not realistic and a spot diameter of d_f = 96 µm, measured directly after the implementation of the machine, is assumed for the experiments. It is likely that this parameter will change over time, which would need to be stabilized in an industrial setup. In the context of this deliverable, it must be clarified to what extent the spot form or intensity distribution plays a role.

1.3 Measurement equipment

Different state-of-the-art measurement and analysis systems were applied to monitor the process results: analyze the effects of laser irradiation on the Si surface, and track the KPIs as summarized in HIPERDIAS deliverable D1.2. In brief, the following measurement and analysis systems were used:

- *ex situ* white light interferometry (WLI) for fast profilometry of microstructures (e.g. test geometry)
- *ex situ* laser scanning microscopy (LSM) for profilometry of small surficial areas and features
- *ex situ* scanning electron microscopy (SEM) for in-depth analysis of surficial features and cross-sections

1.4 Key aspects of laser process

The KPI's can be divided into two categories: Productivity and Quality. Productivity can be described primarily by the absolute and relative energy specific volume. Quality, on the other hand, is described by

the roughness, defects, cracks, edge radius and thickness of the damaged surface layer. In an experimental approach, roughness can be seen as an essential condition for the other KPI's, which is why it can be used as the primary evaluation criterion. In order to understand the approach that was chosen to produce the demonstrator geometry, the central aspects of the laser process with high average power are described and discussed in the following.

1.4.1 Absolute and energy specific ablation rate

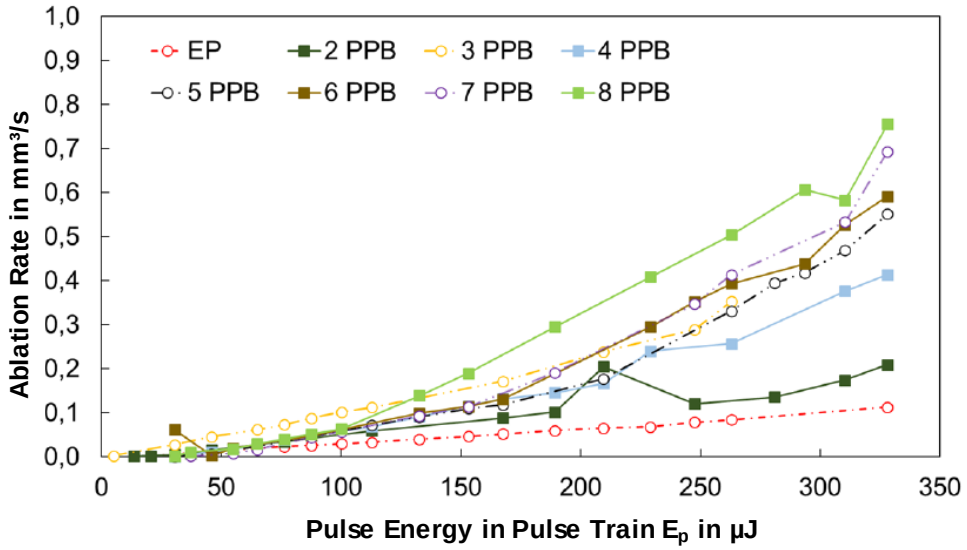

Figure 2: Ablation rate as a function of the pulse energy and pulses per burst (PPB) using a scan velocity of 9 m/s, pulse repetition rate of 1280 kHz and 20 overscans.

The diagram in Figure 2 depicts the experimental results regarding the absolute ablation rate whereby the following trends can be identified: The ablation rate increases with pulse energy (and also fluence, assuming a constant spot diameter for varying pulse energy and average power). Furthermore, the ablation rate increases with the number of pulses per burst. These results confirm the assumptions gathered from the process development with medium average power.
Both factors lead to a maximum ablation rate of approximate 0.8 mm/s which is close to the project goal of 1 mm³/s (KPI #1).

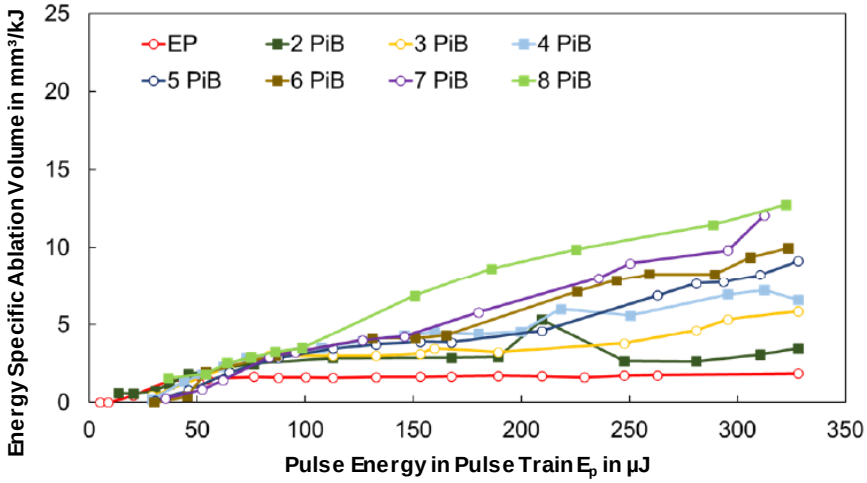

Figure 3: Engergy specific ablation rate as a function of the pulse energy and pulses per burst (PPB) using a scan velocity of 9 m/s, pulse repetition rate of 1280 kHz and 20 overscans.

One of the central findings of the process development in WP2 was an almost linear increase of the energy specific ablation rate when using more pulses per burst (PPB), which was shown for up to 5 PPB. This has been communicated to the HIPERDIAS partners in the early phase of the project with the result, that the Laser was designed to be burst capable with up to 8 PPB. The experimental results that are illustrated in Figure 3 confirm the hypothesis, that an increase is possible beyond 5 PPB. Furthermore, an increase of the energy specific ablation rate can be observed with the use of a combination of burst mode, high average power and high pulse energy. This behavior is very beneficial in order to achieve the project goal regarding absolute ablation rate.

1.4.2 Surface roughness and quality

The beneficial effects of the combination burst mode with more pulses per burst, higher average power and higher pulse energy are however mitigated by an increase of the surface roughness.

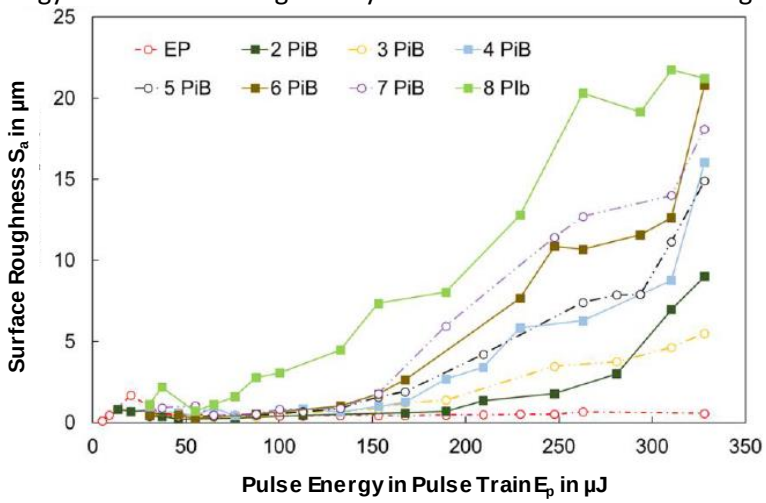

Figure 4: Surface roughness as a function of the pulse energy and pulses per burst (PPB) using a scan velocity of 9 m/s, pulse repetition rate of 1280 kHz and 20 overscans.

It can be obtained from Figure 4 in comparison with Figure 2 and Figure 3 that the increase in surface roughness behaves similarly to the increase of ablation rate. Conclusions on the causes of this behaviour can be drawn from the REM images depicted in Figure 5. When applying single pulses, the surface is very smooth so that the overlap of the scan lines can be obtained. When applying bursts, the surface exhibits irregular structures that are larger when using more pulses per burst.

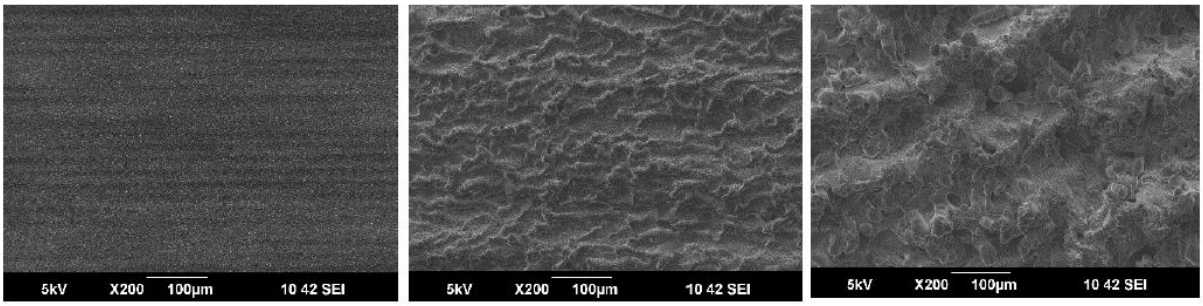

Figure 5: Scattered Electron Microscopy images of the surfaces created with single pulse (left), three pulses per burst and eight pulses per burst using a scan velocity of 9 m/s, pulse repetition rate of 1280 kHz and 20 overscans.

1.4.3 Quality versus Productivity

The identified process characteristics identified here allows us to derive one of the central challenges in the production of target geometry, namely that quality and productivity contradict each other. This tradeoff was not expected, since the experiments in WP2 with a low average power of up to 50 W showed a contrary behavior when using burst mode. A strategy must be found here in order to manage this tradeoff. A possible solution is to use enhanced process strategies that contains multiple steps, e.g. a roughing step and a finishing step. For a roughing step, process parameters must be found that lead to maximum ablation rate with a satisfactory roughness. For a subsequent finishing step, parameters are suitable whereby the roughness is minimized and the ablation rate plays a subordinate role. Besides other process parameters which can influence the process, the scanning speed can primarily be used as an adjustable value as is exemplarily shown in Figure 6 for single pulse

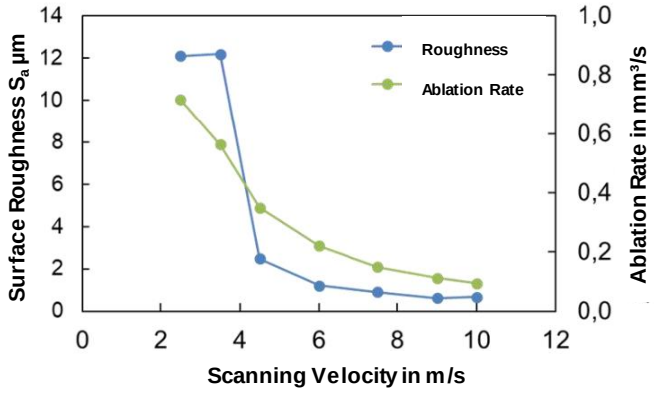

Figure 6: Behavior of surface roughness S_a and ablation rate as a function of the scanning velocity for single pulse ablation with an average power of 430 W and pulse repetition rate of 1280 kHz.

2 Analysis of laser process w/ high average power on reference sample

In the following, the overall USP ablation process of silicon and the corresponding KPI's are evaluated using the demonstrator geometry that incorporates all the features of a later product. In a first step, the individual details and features are described and how they are measured or determined. In the following step, these are evaluated with regard to the laser process. Furthermore, the potential of a multi-step process is discussed in order to achieve satisfactory results using high average power. This includes a 1st set of viable process parameters for roughing and finishing that demonstrate feasibility. The consequent summary of KPI's showing promising potential regarding the project goal but also indicating further potential for the ablation process of silicon.

2.1 Determination and measurement of characteristic geometric features

As result of the findings in WP2.4 "upscaling", the demonstrator geometry was processed using the optimal process that was known up-to-date using the 500 W-demonstrator at the IFSW laboratory. This process was optimal to the extent that it combined a high absolute ablation rate (KPI #1) and comparatively smooth surfaces (KPI #4). The surface roughness was evaluated as too high immediately after the end of the process by visual inspection. As a result, it was decided to apply a post-processing (smoothing) step and slightly modify the demonstrator geometry in order to maintain comparability of the surfaces.
As can be seen in Figure 7, the levelled surfaces marked with A and A* are of particular interest, whereby A* is taken as the post-processed counterpart of A. This also applies to the areas B and B*, which represent the chamfer surface.

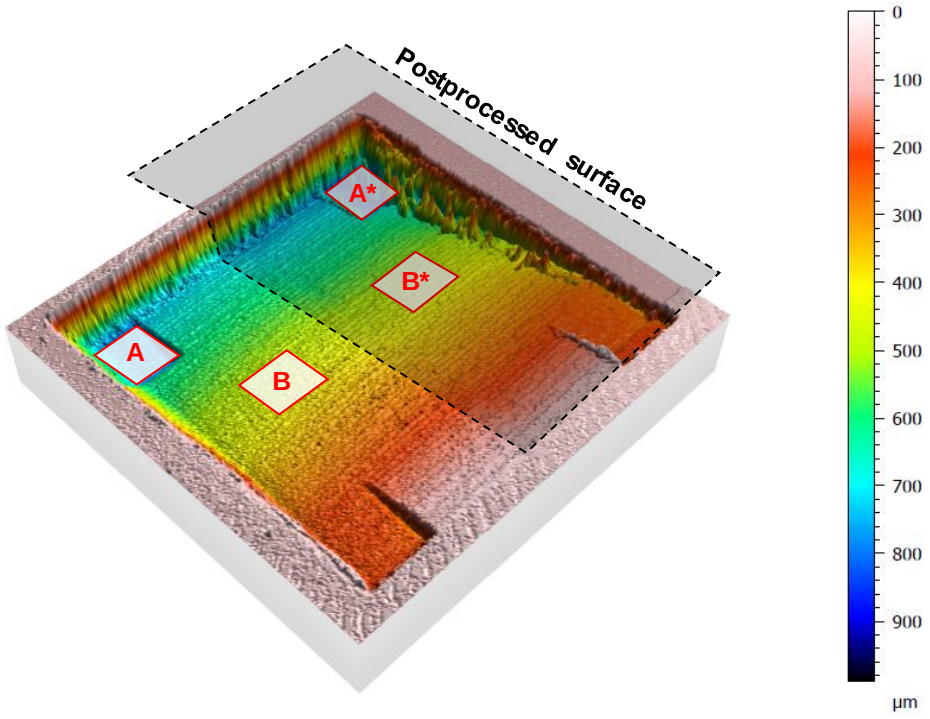

Figure 7: Geometry created with high average power using efficient femtosecond 7-pulse burst and postprocessing step with single-pulse on one-half of the geometry, topography measured using white light interferometry (WLI). Highlighted areas of interest.

The increased roughness on the surface has a direct effect on the measurability of the surface as it leads to reduced measurement signal, especially at edges. Therefore, the surface is interpolated locally by using the surrounded measurements signals which are sometimes in questionable reliability. This method is locally not trustworthy and eventually lead to spikes as result from false interpolation. As a result and contrary to the measurement procedure for the reference geometry, the areas of interest have been re-measured using laser scanning microscopy (LSM) that exhibits a high lateral and axial resolution. By principle, the process is more robust in the acquisition of rough surfaces. However, this has the disadvantage that a measurement takes a very long time so that the complete structure cannot be recorded. The detailed measurements of the “roughed” surfaces in the areas if interest A and B are depicted in Figure 8 and Figure 9, respectively. The post-processed surfaces in the areas of interest A* and B* are shown in Figure 10 and Figure 11.

It can be observed that as smoothing step can have a significant impact and lead to a reduction of roughness from Sa = 5.04 µm to Sa = 2.71 µm. This also leads to a macroscopically visible change of the surface reflectivity. Unfortunately, the post-processing can lead to defects / holes in the surface such as 4 defects in Figure 10 and 1 defect in Figure 11 which in average corresponds to 5 defects per mm².

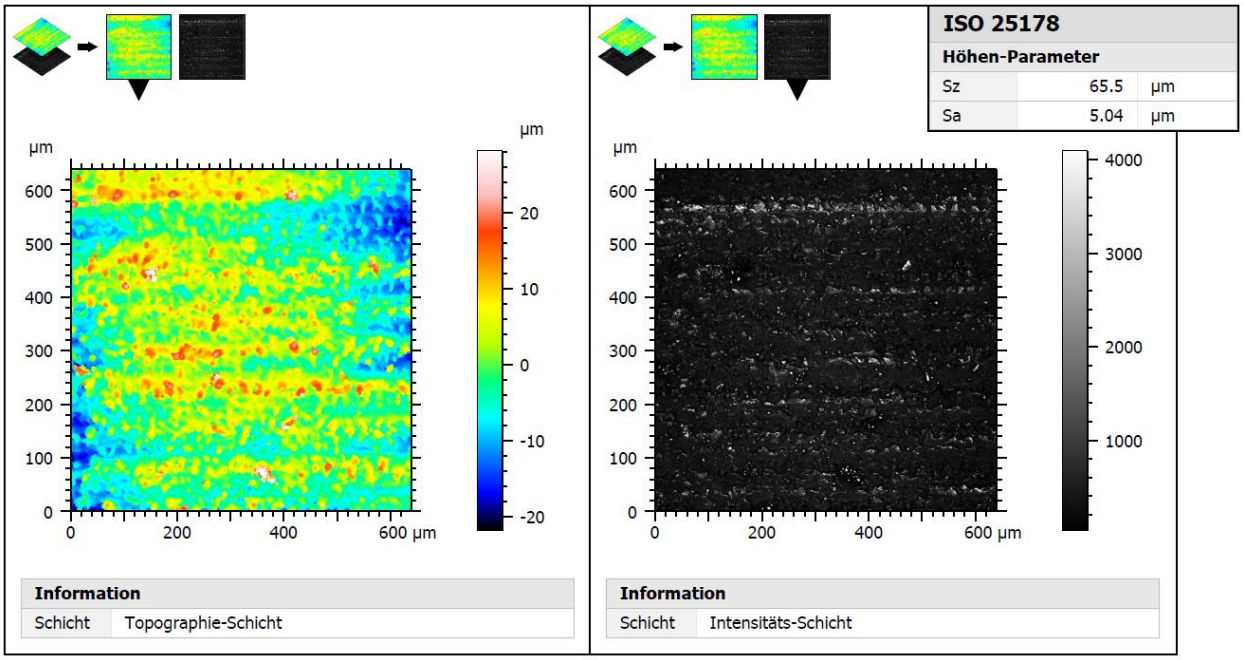

Figure 8: Topography (left) and corresponding measurement intensity (right) of the Plane surface without postprocessing (Area A), measured using laser scanning microscopy (LSM). Roughness parameters according DIN EN ISO 25178 (inset).

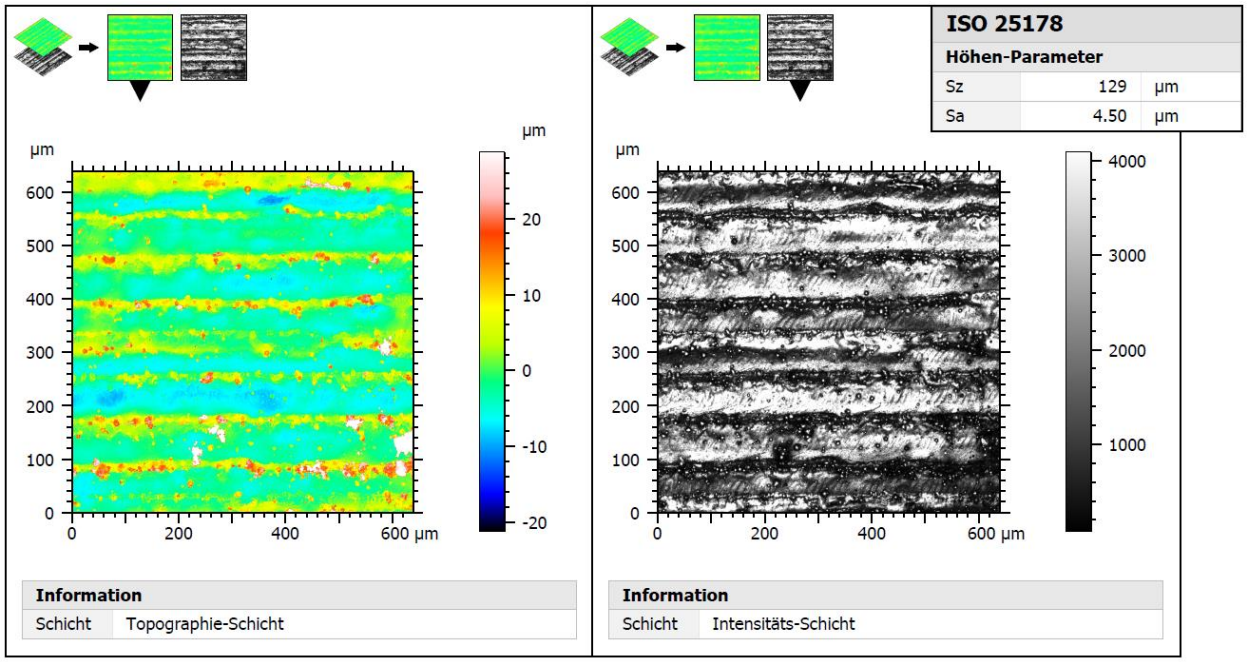

Figure 9: Topography (left) and corresponding measurement intensity (right) of the chamfer surface without postprocessing (Area B), measured using LSM. Roughness parameters according DIN EN ISO 25178 (inset).

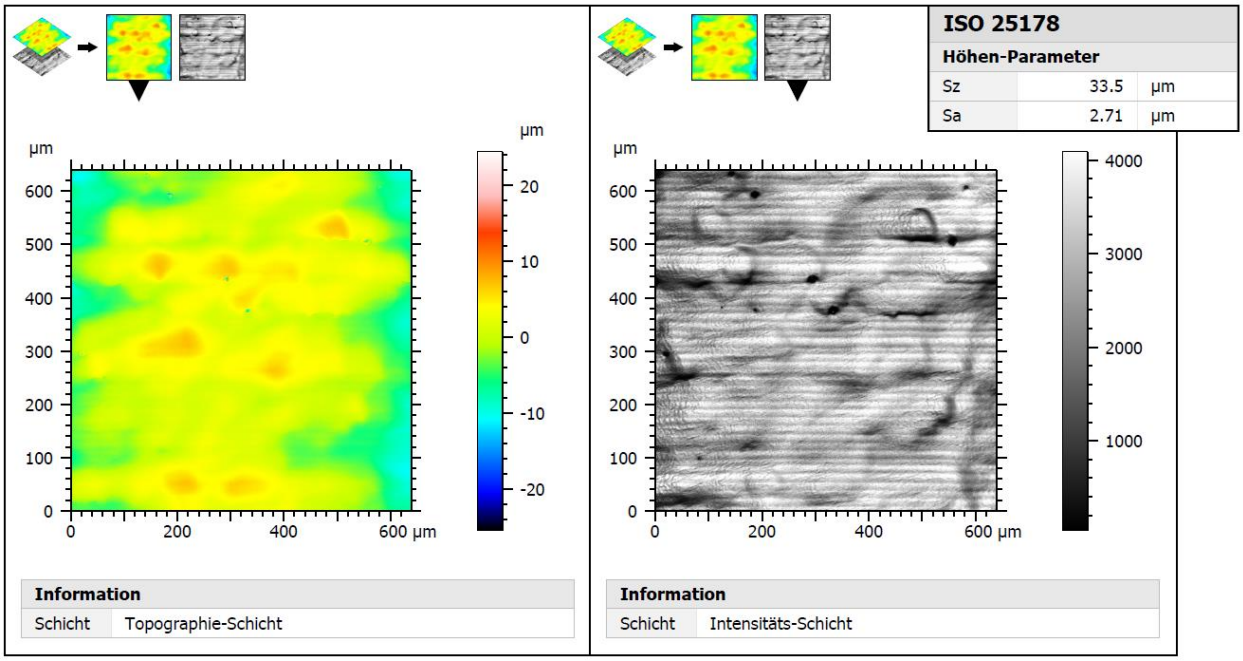

Figure 10: Topography (left) and corresponding measurement intensity (right) of the Plane surface after postprocessing (Area A), measured using LSM. Roughness parameters according DIN EN ISO 25178 (inset).*

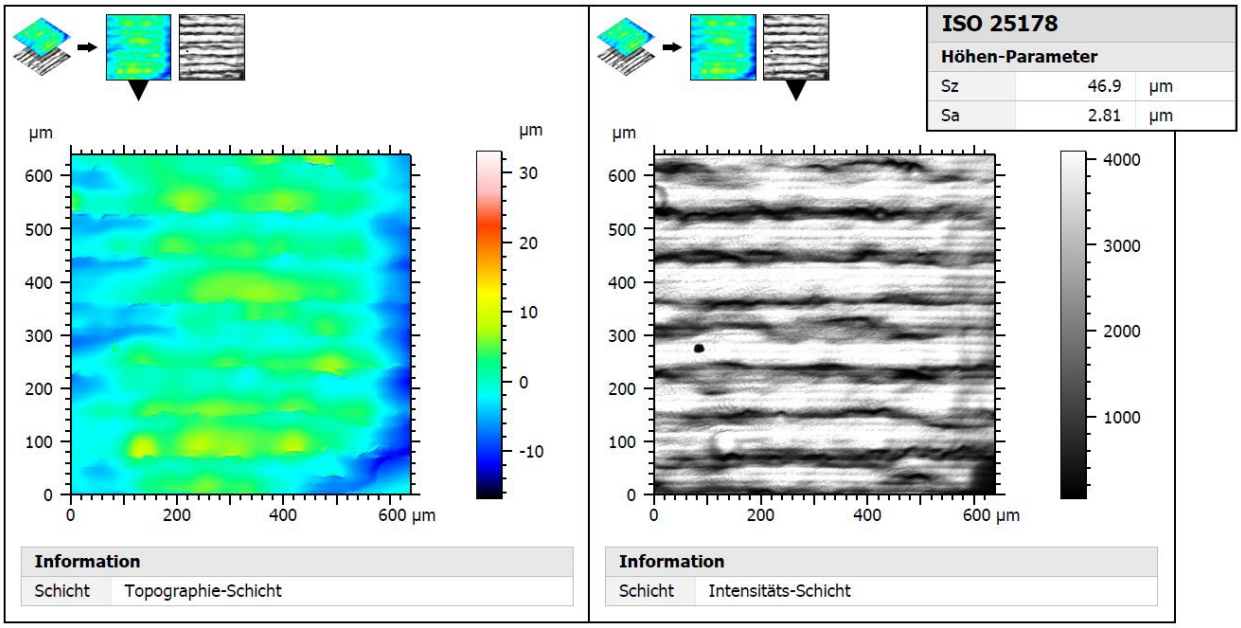

Figure 11: Topography (left) and corresponding measurement intensity (right) of the chamfer surface after postprocessing (Area B), measured using LSM. Roughness parameters according DIN EN ISO 25178 (inset).*

A further important aspect is the minimal achievable edge radius as it is an important prerequisite for the production of precise structures. For evaluation, the four corners of the demonstrator geometry are used. The topography in the concerned areas C, D, E, and F have been transformed to contour objects using a threshold value that defines whether a measurement pixel is inside or outside the structure. Subsequently, a quarter circle is fitted to the pixel coordinates that define the corresponding contour. The radius of the circle is then taken as the edge radius. As shown in Figure 12, the radii varies in a range from 48.1 µm to 87.9 µm, with an average of 74.1 µm that is used as value for KPI evaluation.

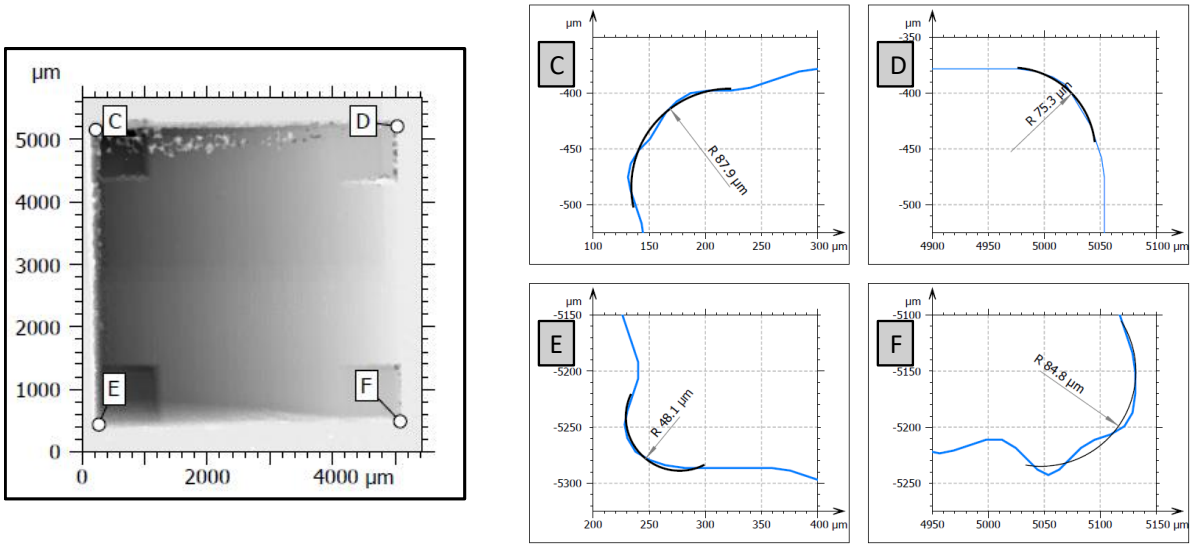

Figure 12: Illustration of the measurement positions for edge radii (left), extracted contour for positions C to F including fit and determination of radius (right).

The angle of the sidewalls is of interest as they are an essential design attribute. For evaluation, all data in the rows of the topography measurement in the area G which is limited by the black horizontal lines depicted in the illustration in Figure 13 is averaged to a single contour. Two lines can be fitted to segments of the contour: one on the surface and one on the inclined surface. For this demonstrator geometry a relative angle of 80.2° can be determined.

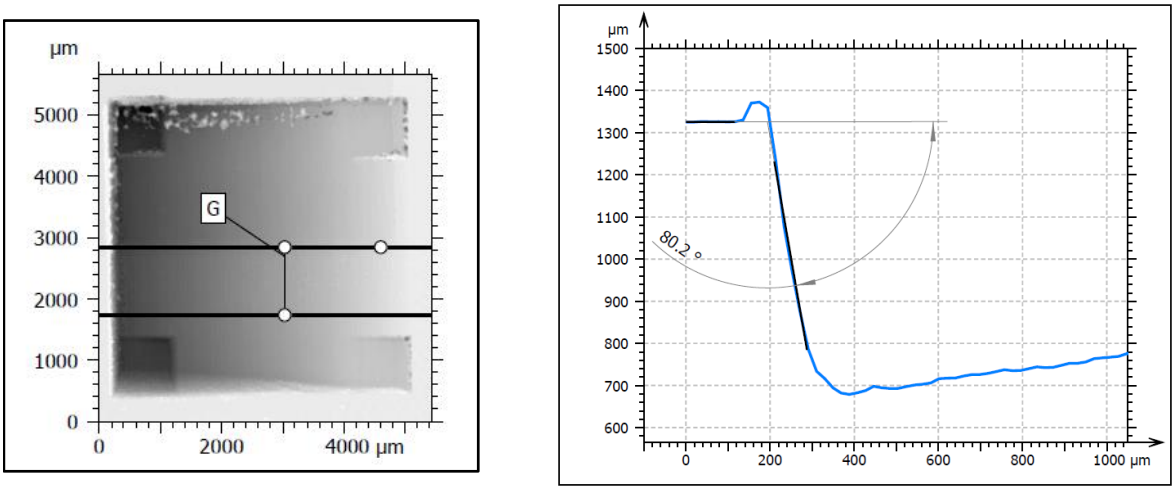

Figure 13: Illustration of the corridor for the measurement of edge steepness (left), average of all line profiles and determination of edge steepness.

The measurement of form deviation is comparatively complex and involves several steps in the processing of data. As can be identified in Figure 14 for the roughed surfaces and in Figure 15 for the post-processed surface, the inclined parts of the geometry have to be extracted. There are several factors that make it necessary to filter the surface as spatters, measurement artifacts, roughness and waviness with a low wavelength strongly influence the result. In order to obtain conclusive results, the cutoff wavelength of the gaussian filter used must be adjusted precisely which in this case is set to λ_{cutoff} = 250 µm. The S_z-value according EN ISO 25178, which is applied to the entire measuring area, corresponds to the peak to valley deviation can be taken as the value for the form deviation. Here, a S_z = 22.0 µm can be evaluated for the roughed surface and a S_z = 26.9 µm for the post-processed surface along the respective areas of interest.

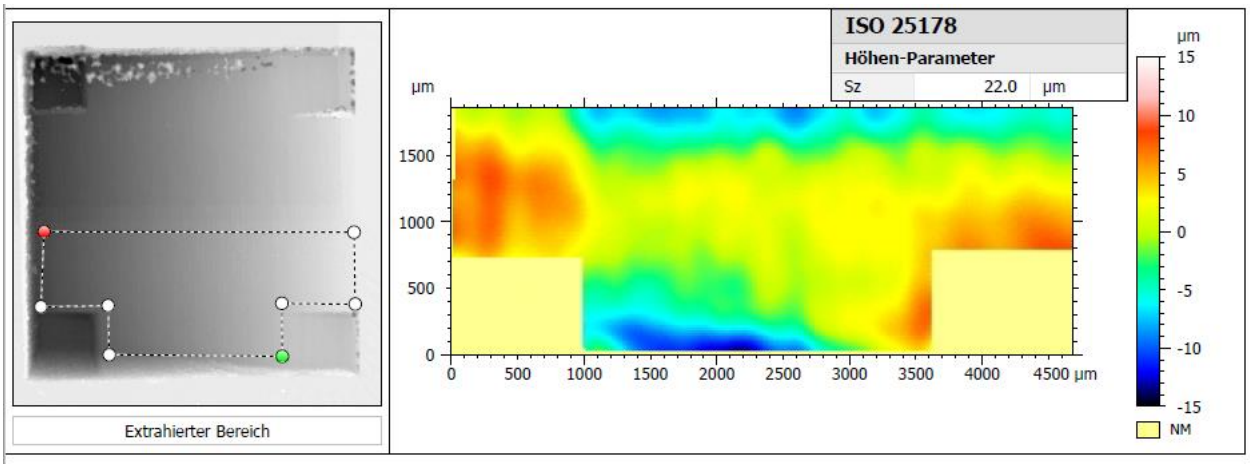

Figure 14: Area of interest (aoi) for the measurement of shape deviation of roughed surfaces (left), levelled topography in the aoi including applied wavelength filter with λ_{cutoff} = 250 µm (right), Peak-to-valley of surface corresponding S_z according DIN EN ISO 25178 (inset).

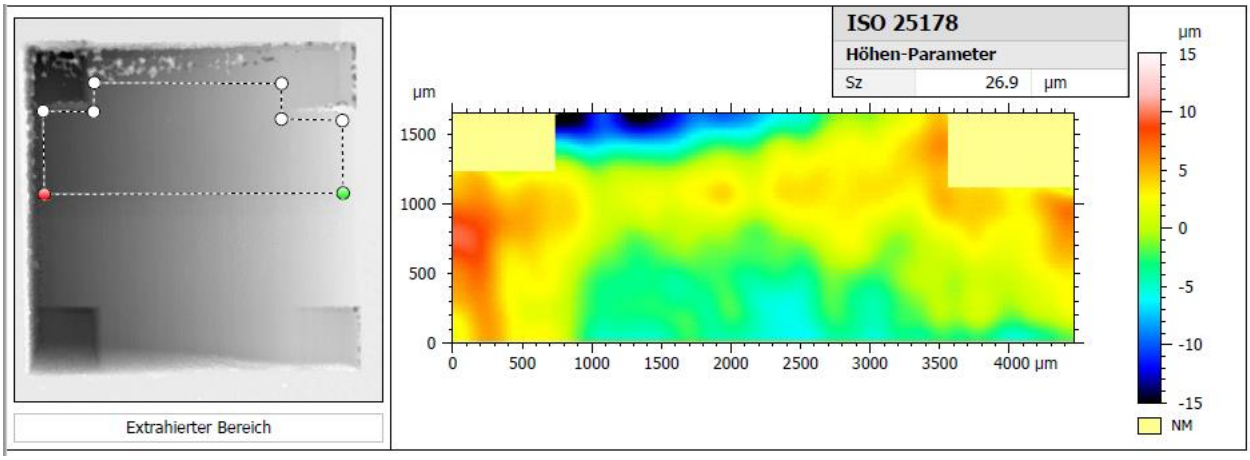

Figure 15: Area of interest (aoi) for the measurement of shape deviation of postprocessed surfaces (left), levelled topography in the aoi including applied wavelength filter with λ_{cutoff} = 250 µm (right), Peak-to-valley of surface corresponding S_z according DIN EN ISO 25178 (inset).

2.1.1 Discussion and evaluation of experimental results

In the following, the aspects that have been evaluated using the demonstrator geometry shown in Figure 7 and the detailed measurements and evaluations shown in Figure 8 to Figure 15 are now discussed with regard to the laser process and primary influencing parameters.

2.1.1.1 Roughness

The roughness was strongly increased during the trial experiments for the demonstrator geometry. Therefore it was decided to test a smoothing – roughing strategy whereby half of the geometry was left in its "roughed" state. The second half was treated with a parameter that promised to result in very smooth surfaces (known from experiments on pristine, polished silicon) with the cost of a low efficiency and therewith productivity.

The very efficient process used for the rough geometry is most likely a process where thermal aspects play a significant role. They cause very high roughness of up to S_a = 5.0 µm on "roughed" surfaces which can be reduced to Sa = 2.7 µm using a smoothing process. Desirable would be a roughness of below S_a = 0.5 µm that has been observed at the reference geometry. Note that in principle, it is possible that the measurement method plays a role here. Significant differences, however, are unlikely since both WLI and LSM have a measurement resolution far in the sub-µm.

For the "roughed" and "smoothed" state, an increased waviness can be observed especially on the chamfer surface. Here, the post-processing step process significantly reduces roughness and micro-roughness with remaining waviness.

2.1.1.2 Shape deviation

The cutouts as obvious form of shape deviation have not been structured on purpose and shall remain as leveled planes because of several reasons:

A comparison of the raw processed surface with the post-processed surface should be possible using the demonstrator. Further, cutout areas and leveled planes exhibit different sizes than originally defined: As it is essential that the levelling works in principle and the absolute size of the levelled surfaces is of minor importance, the precise adherence to the size was given little consideration.

Regarding shape deviation, it is of significant importance that the chamfer geometry is producible with high average power. Several factors are known that could lead to unsteady laser process and hereupon a severely deformed chamfer geometry, e.g. an inhomogeneous intensity profile of the focused laser beam along the propagation axis, the irregular form of the laser spot within the focus (as addressed in the introduction) or insufficient stability of average power and pulse energy over time. Apparently, the laser process is sufficiently stable to enable the processing of a relatively uniform chamfer geometry. In this state of development, a shape deviation of S_z = 26.9 µm is acceptable but must further be improved.

The factors described in the previous sentences are also applicable on the leveled surfaces but are more critical. It can be seen as the creation of a chamfer geometry and a second, subsequent chamfer geometry that results in an even surface.

2.1.1.3 Defects

The post-processing step is likely to induce micro-defects in the surface in the order of magnitude of 5 per mm². The assumption is reasonable, that the success of smoothing is dependent of the initial roughness of the rough surface. Here, optimal processes must be found for roughing and post-processing (smoothing).

For the first demonstrators, critical holes could be observed at the edges for which the exact formation mechanism is still unknown. Therefore it was hard to predict before the upscaling whether the effect would occur at high power levels as well. Fortunately, the efferent roughing process and the smoothing process applied here do not lead to such holes at the edges. Further, the smoothed surfaces appear to be free from cracks.

2.1.1.4 Edge radius

The edge radius is varying in a comparatively large range from $r_e = 48.1$ µm to $r_e = 87.9$ µm. The primary source for the variation is likely to be the roundness of the focused laser spot. Influencing factors are the parameters for the extraction of the profile from the topography as well as the resolution of the measuring device. Furthermore, ablation products that are deposited on the surface can slightly affect the measurement result. An average $r_e = 74.1$ µm is sufficient for most geometries.

2.1.1.5 Edge steepness

The high edge steepness with α_e = 80.2° is very comparable to the α_e = 80° of the reference geometry. This could be expected as the single pulse energy as the primary influencing factor had approximately the same value.

2.1.2 Evaluation of KPI's and conclusion

The findings of the previously discussed demonstrator in comparison with the reference demonstrator geometry can be summarized in brief by evaluating the KPI's listed in Table 3. It should be noted that average removal rate and roughness are the most significant characteristics of the process.

Table 3: Key Performance Indicators evaluated using the demonstrator geometry crated with the ablation process parameters each for low average power (benchmark; status @ end of WP2.1) and high average power (status @ end of WP2.4)

Key Performance Indicator	Symbol	Unit	Target Value	Value (reference)	Value (500 W Demonstrator)
KPI #1: average ablation rate	$\dot{V}$	mm³/s	≥1	**0,0574 (P_{av} = 20 W)**	**0,55 (P_{av} = 430 W)**
KPI #2: peak ablation rate	$\dot{V}_{max}$	mm³/s	≥3	-	-
KPI #3: shape deviation	δ_S	µm	≤10	**<10**	**22**
KPI #4: average surface roughness	S_a	µm	≤1	**<0,5**	**<3**
KPI #5: thickness of surface damage	l_d,s_d	µm	≤1	**<1**	-
KPI #6: Surface defects > 1 µm	–	1/mm²	none	**none**	**5**
KPI #7: min. achievable edge radius	r_e	µm	≤ 200	**60**	**74**
KPI #8: max. edge-steepness	α_e	degree	≥ 70	**80**	**80**

In addition, the following essential insights can be obtained that induce further potential for the development of post-processing strategies:

- The project goal of achieving an average ablation rate of 1 mm³/s can most likely be obtained.
- Using high average power and high efficiency leads to rough surfaces but can be smoothened by using adapted laser parameters in a smoothing post-processing step.
- Thereby, a high initial roughness (before smoothing process) is likely to lead to surface defects and holes at post-processing.
- A certain amount of waviness remains, especially on chamfer surfaces, leading to an increased value for KPI #4. Here, the scanning velocity and hatch distance are most likely to have a significant influence.
- Use LASEA software for the creation of the demonstrator geometry, the chamfer surface in particular

3 Summary

Within the context of this deliverable, the laser process is evaluated on the basis of the demonstrator geometry, which exhibits the relevant features of later products. This is different to the fundamental process development that relies on flat rectangular structures.

The parameters identified in the fundamental process development to meet the KPI's were translated into the system requirements that served as input for the development of laser and machine. The deliverable contains a comparison of the input values and their degree of fulfillment for the established system.

In order to understand the approach that was chosen to produce the demonstrator geometry, the key aspects of the laser process with high average power are described and discussed. Here the central statement is that for high average power the parameters that lead to high productivity also lead to a deterioration of the surface quality. In order to manage this tradeoff, a multi-step processing is proposed that contains an efficient roughing step and a subsequent finishing step that is less efficient but allows the achievement of the quality.

As a central part of this deliverable, the results of the measurements of the demonstrator geometry are investigated in detail with regard to measurement reliability and the origin and processing of measurement data. In addition to the measuring equipment used in previous work, laser scanning microscopy was used which provides an even more accurate insight into the quality and microstructure of the sample surface. Based on this measurements, the relevant quality KPI's are evaluated and discussed: Roughness, shape deviation, Defects, edge radius and edge steepness. Furthermore, insights into the process could be gained from which improvements can be derived.

The overall results are promising but show further potential for improvement. Regarding the main objective of the project, to achieve an absolute removal rate of 1 mm^3/s, it can be confidently assumed that this can be achieved with the 1000 W system.